Circular Polarisation for Optical Pumping in TRINAT
Winter 2020

Anastasia Afanassieva

May 4, 2020

1 Introduction

At TRINAT (TRIumf's Neutral Atom Trap), nuclei are spin polarised and allowed to beta decay in order to make measurements of the beta asymmetry with respect to spin. Circularly polarised light is directed onto the trapped atoms in order to optically pump the atoms driving them to the desired spin polarised state.

When making beta decay measurements, the nuclear spin is flipped between two opposing states. This is done in order to take an average of the measurements made by two detectors on opposite sides of the trap, allowing for more precise measurements of the beta decay. The flipping between two spin states requires two opposing orientations of circularly polarised light. Previously, this was achieved using a Liquid Crystal Variable Retarder (LCVR). A key component of this term was the characterisation of the Transient Nematic Liquid Crystal (TNLC) which would replace the previous LCVR. A few key measurements of these devices included the operating voltages and the resulting circular polarisations.

We found that we were able to improve the circular polarisation by an order of magnitude to 0.99996 by installing an additional linear polarizer to the optical pumping line. This linear polarizer would be added with a motorized rotation stage from Thorlabs' Elliptec range of products. Due to unforeseen lab closure, we were not able to install the motorized stage on the beam line. Code was written and a plan for how we would be able to install the stage were made and should be done once the lab is reopened.

We worked on optimizing fiber launching into the optical fiber that provides light to the optical pumping beam line. We were able to improved the percentage of the light transmitted through the fiber. The new laser diode that was installed prior to our measurements resulted in a 3x increase in the power available to the optical pumping light than was previously recorded. This allowed for a decrease in the amount of time it would take to spin polarise the nuclei in the atom trap.

Finally, we were able to predict the improvement of the nuclear spin polarisation given the improvements in power and light circular polarisation over the term.

Contents

2 Measuring Circular Polarisation

In order to the measure the circular polarisation, S_3, we need to measure the power of the light coming out of the QWP using a diagnostic polarizer (Figure 1). We need to make this measurement at 4 different angles: Where S_1I_x and S_1I_y are 90° apart, and S_2I_x and S_2I_y are 45° from S_1I_x and S_1I_y respectively (Figure 2). It was found that it was unimportant to measure the power using S_{1x} and S_{1y} as the minimum and maximum locations respectively. As long as the relative angles follow Figure 2, the results should be the same.

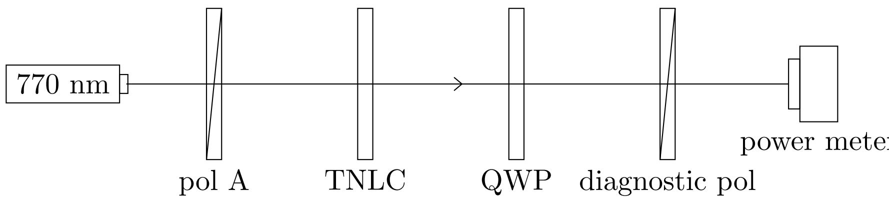

Figure 1: QWP and S3 test setup

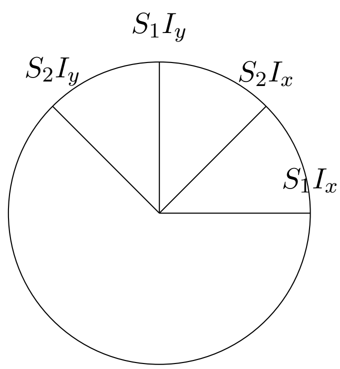

Figure 2: Orientations for S3 calculation

We can then use these measurements to find the two parts of the linear polarisation S_1 and S_2 (Equations 1 and 2). We can then use those to measurements to find the total linear polarisation S_{lin} (Equation 3) and then finally the circular polarisation S_3 (Equation 4).

$$S_1 = \frac{S_1I_x - S_1I_y}{S_1I_x + S_1I_y} \tag{1}$$

$$S_2 = \frac{S_2I_x - S_2I_y}{S_2I_x + S_2I_y} \tag{2}$$

$$S_{lin}^2 = S_1^2 + S_2^2 \tag{3}$$

$$S_3 = \sqrt{1 - S_{lin}^2} \tag{4}$$

3 Twisted Nematic Liquid Crystal Overview

The Transient Nematic Liquid Crystal Rotator (TLNC) from Meadowlark Optics takes as input linearly polarised light. As output, the TNLC will either rotate the axis of polarisation by 90° or will leave the light unchanged. This is achieved through the twisted structure of liquid crystal shown in Figure 3. [3] Applying a voltage across the TNLC, the molecules align themselves with the electric field and eliminate the birefringence of the crystal, allowing the light to pass through with no rotation.

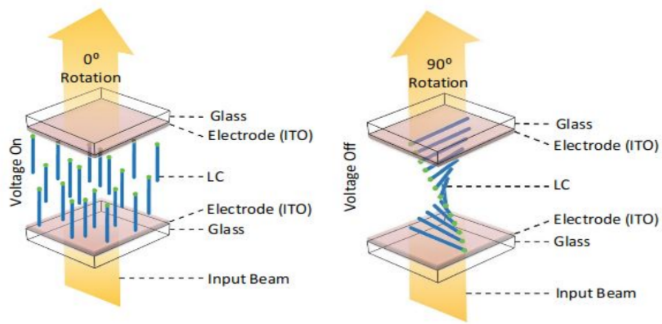

Figure 3: Meadowlark Figures of the Twisted Nematic Liquid Crystal

3.1 Measuring Time Dependence

Extinction Time Measurements

I am measuring the time it takes for the polarisation to flip by 90 degrees. This will give an idea of how long it should take to achieve circular polarisation once we install the Quarter Wave Plate (QWP).

In order to make this measurement, the laser enters a linear polarizer, then enters the TNLC then passes through a second, diagnostic, polarizer (Figure 4). The diagnostic polarizer is at an angle such that it is 90 degrees from the output of the TNLC rotator. Once the light is fully rotated, the intensity coming out of the diagnostic polarizer should be at its minimum. Using an oscilloscope, the power output can be measured as a function of time from when the voltage switched states along the TNLC.

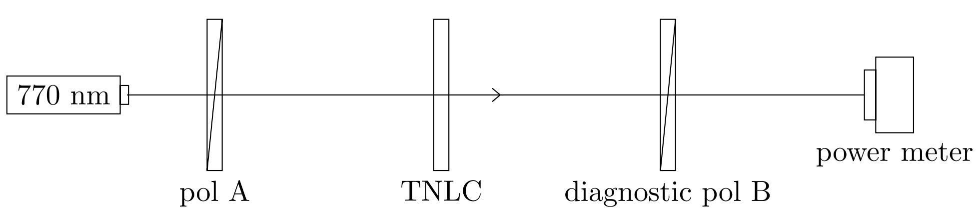

Figure 4: Extinction test setup

3.1.1 Waveform generator

The TNLC was controlled using the Meadowlark D5020 Liquid Crystal Controller with the CellDrive5000 program provided. There were two types of waveforms that I was using:

1. **Square Wave** This function simply switches from low to high voltage at whichever period you chose. The waveform generator sending a voltage to the TNLC itself generates a 2kHz Square Wave at the desired low and high voltages. We cannot put a DC voltage without damaging the device but the D5020 Liquid Crystal Controller manages this for us.

2. **Transient Nematic Effect (T.N.E.)** This wave function is similar to the Square Wave, except that instead of going from the high voltage to low voltage state directly, it will first overshoot passed the desired low voltage and then after a certain amount of 'TNE time' it will return to the selected low voltage state. The goal in this function is to decrease the time it takes for the liquid crystal to relax to its twisted shape and thus decrease the time it takes to get the greatest extinction.

3. **External Input** Another way of controlling the voltage going to the TNLC, is providing an external input. In this method, the voltage input from a function generator connected to the I/O port will be doubled and applied to the TNLC. (Ex: If you send a 0 to 5V square wave to the I/O port, the TNLC will have a 0 to 10V square wave applied.) **Note: To use this feature close the CellDrive2000 Software**

4. **Threshold** This feature allows you to chose a low voltage and a high voltage setting with the CellDrive2000 software. The controller will then read the input voltage through the I/O port. If the voltage is below 5V the low voltage will be applied to the Liquid Crystal. If the voltage is above 5V the high voltage will be applied.**Note: To use this feature close the CellDrive2000 Software once the high and low voltages have been configured.**

5. **Sync Out** This feature cannot be used with the External Input and Threshold features. Used in combination with the Square Wave or T.N.E. waveforms, Sync Out sends a pulse through the I/O ports at a specified time in the waveform's period. I used this setting to trigger the oscilloscope. When the voltage changed from 10V to 0V a pulse would be sent triggering the oscilloscope and taking data to measure the time dependence of the extinction or circular polarisation. For best results I made the sync out pulse time as long as the CellDrive would allow for otherwise the oscilloscope was not able to see the pulse.

4 TNLC #1 (1.273-10V)

4.1 Voltage v. 90° Rotation

In characterizing the liquid crystal device we found that there was not a perfect 90° rotation when the voltage is changed from 0V to 10V. With this TNLC, the 90 ° flip occurred with a low voltage: 1.273 V and a high voltage: 10.0V, when light enters with polarizer A at 164°10. Figure 5 shows the deviation from a 90° light rotation. We can see from the figure 6 that the TNLC is very sensitive to voltage changes around 1.273 so this angle is critical. Lina Nguyen's April 2019 report found that the flipping voltage was 1.408V so it would be advised to conduct a periodic check, ensuring the rotation is still 90° at 1.273V.

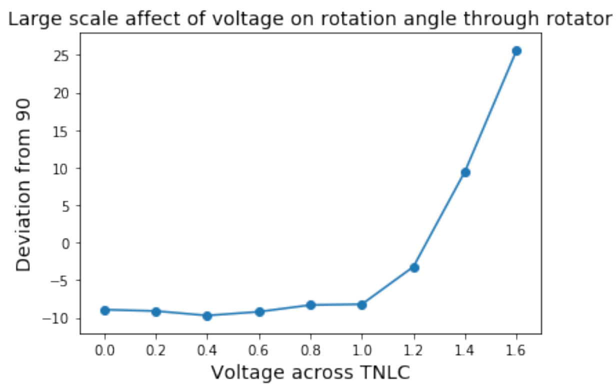

Figure 5: Graph showing how the voltage applied to the TNLC affects the rotation angle over a large voltage scale

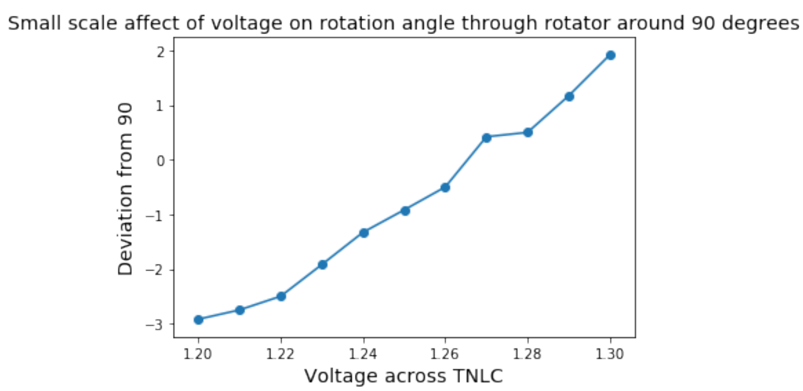

Figure 6: Modifying the voltage applied to the TNLC on a smaller scale to find the optimal voltage to be applied

4.2 Extinction Time Measurements

The measurements taken in Figures 7 and 8 show two different wave forms. Figure 7 uses a square wave function from 10V to 1.273V. Figure 8 uses the T.N.E function described in Section 3.1.1 with a T.N.E time of 50ms and a T.N.E. Voltage of 0V. As can be seen comparing Figures 7 and 8, using the TNE waveform allowed for a decrease in time from 90ms in the square wave to 40ms using the TNE wave.

Shown in Figure 9, the extinction time from a low to high voltage happens much faster than the high to low voltage transition. This is because there is no electric field to force the molecules back into there twisted state. This transition relies on the interaction forces between the neighbouring particles, a much weaker force than the electric force.

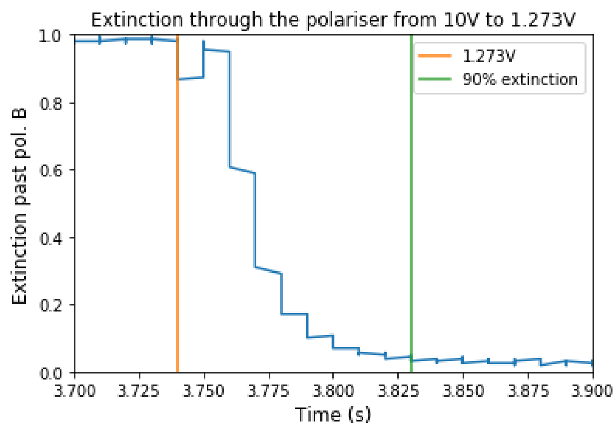

Figure 7: Extinction from 10V to 1.273V state using the square wave function

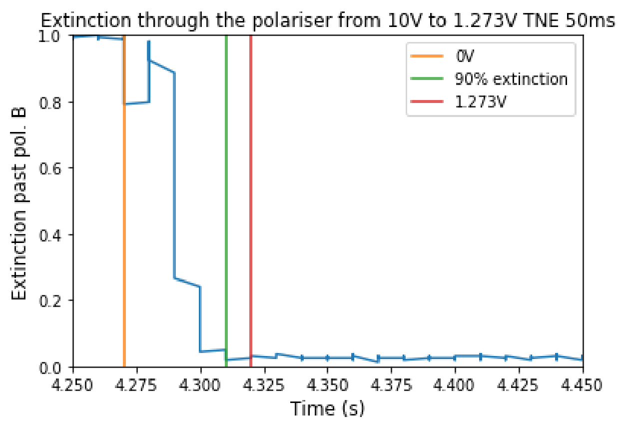

Figure 8: Extinction from 10V to 1.273V state using the TNE function going to 0V for 50ms.

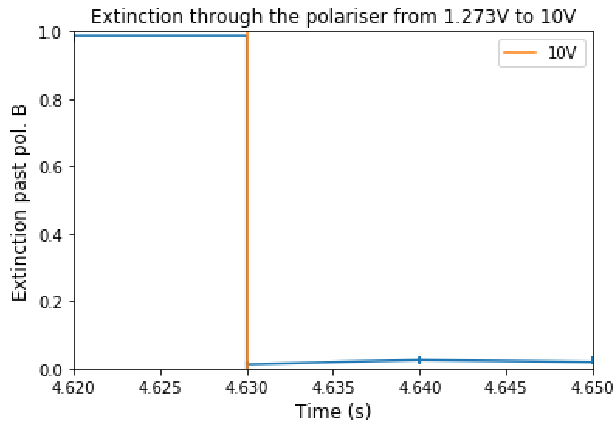

Figure 9: Extinction from 1.273V to 10V using the square wave function

4.3 Circular Polarisation v. QWP angle

4.3.1 Optimising Quarter Wave Plate

Now we need to install a Quarter Wave Plate (QWP) in order to circularly polarise the light. In order to get the best circularly polarised light, the linearly polarised light (from TNLC) must be at 45° from the QWP fast-axis.

To optimize, the QWP is rotated and S_3 is measured for a number of angles in order to find the QWP orientation that will give the best S_3.

4.3.2 Results

Initially, I was using the "Mdlk RCQ-100-768 #8" Quarter Wave Plate, this gave the plot shown in Figure 10, the best S_3 I was able to achieve was around 0.9983 which is worse than in Figure 30 of Lina's Report where she achieved an S_3 up to an order of magnitude higher.

We then tried a new QWP the "Meadowlark D2180" and found better S_3 as shown in Figure 11. From now on unless otherwise stated this is the QWP used.

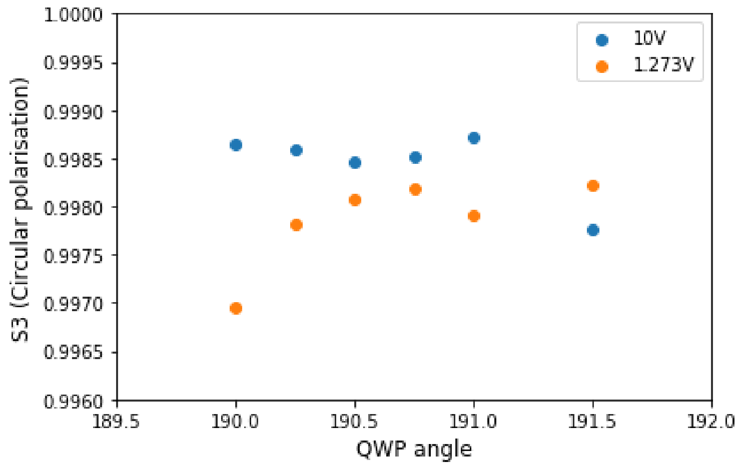

Figure 10: S_3 v. QWP angle for Mdlk RCQ-100-768 #8

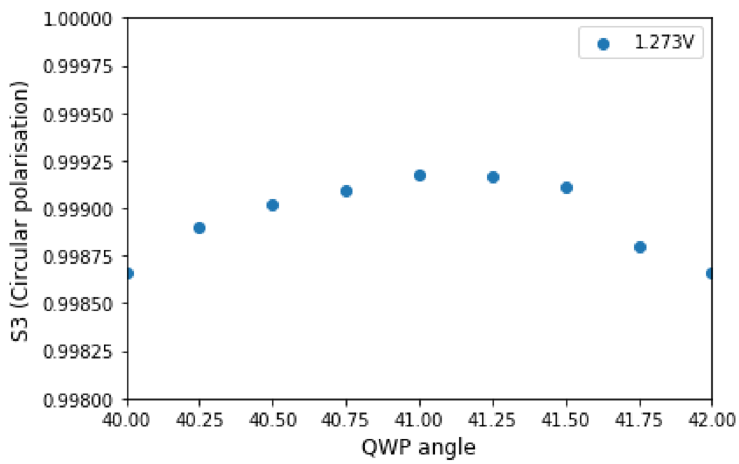

Figure 11: S_3 v. QWP angle for Mdlk D2180

4.4 Circular Polarisation as a Function of Time

The final thing to look at with this polarizer was the S_3 as a function of time to see how quickly we could get the best possible circular polarisation.

The S3 as a function of time using the “Meadowlark D2180” QWP is shown in Figure 12, we can see the S3 creeping up over the seconds time scale. To make this measurement I used the TNE function with a TNE time of 50 ms and a TNE voltage of 0V.

I wanted to see if this same effect could be found using the QWP from the trap. So Figure 13 shows the S3 as a function of time measurement using the “I12117” QWP and we can see that the scale is much smaller than Figure 11. To make this measurement I used the TNE function with a TNE time of 50 ms and a TNE voltage of 0V.

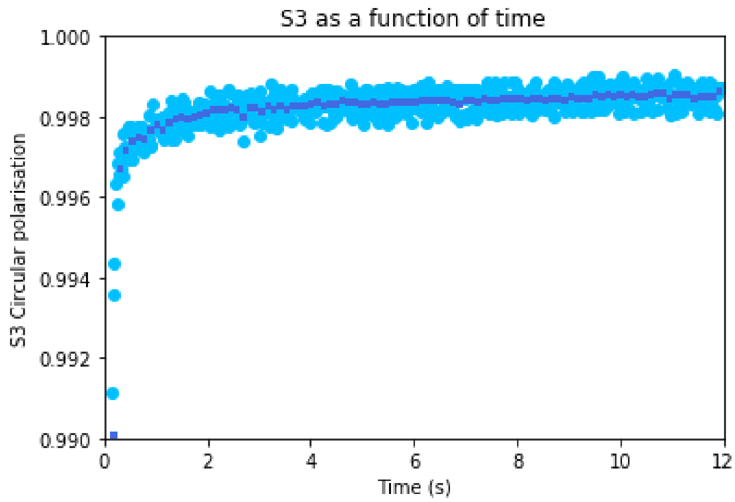

Figure 12: S3 as a function of time with QWP:Meadowlark D2180, angle:41 degrees, temperature: 25.9

Note: The setup for this measurement is the one shown in Figure 1 above.

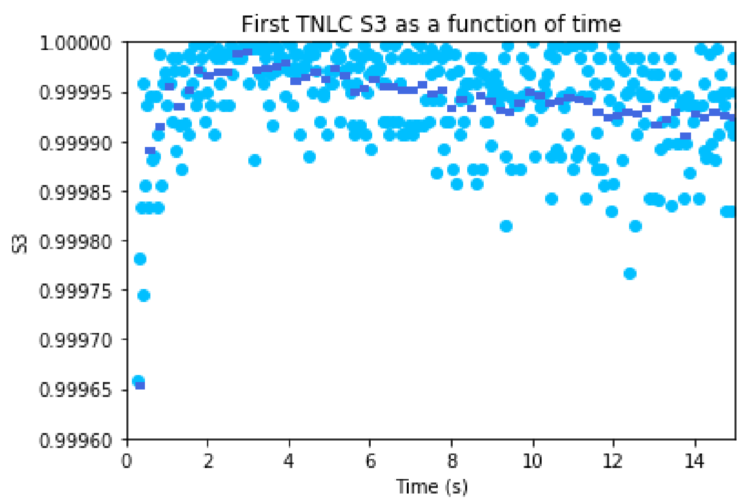

Figure 13: S3 as a function of time with QWP: Meadowlark I12117, angle:137.75, temperature: 25.9

5 TNLC #2 (0-10V)

5.1 Voltage v. $90°$ Rotation

5.1.1 Polarizer A angle

When installing the new TNLC the first thing to do was check the optimal angle for polarizer A in Figure 4's setup. In Figure 14, I adjusted linear polarizer A and measured the extinction ratio of the outgoing linearly polarised light by rotating the diagnostic polarizer B by 90 degrees and dividing the smaller power reading by the larger reading. The optimal angle shown in Figure 1 was 158 degrees.

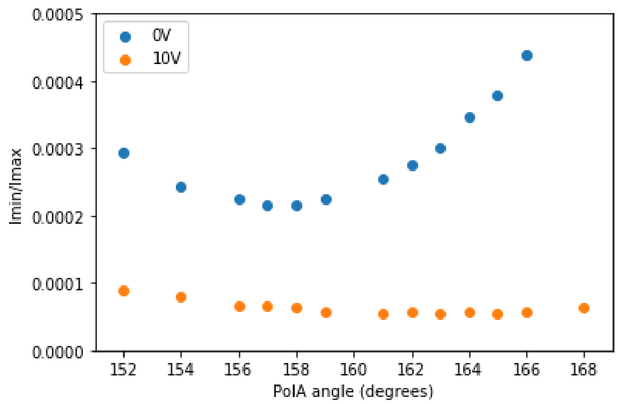

Figure 14: Extinction v. polarizer A angle for the 0V and 10V state to try to optimize the linearly polarized light incident on the TNLC.

5.1.2 90 degree Rotation

In the other TNLC, the 90 degree flip between the low and high voltage state occurred between 1.273V and 10V, so for this TNLC it was also important to check where the 90 degree flip occurred. From 0V to 10V the flip was 89 degrees instead of the desired 90. To account for this I adjusted the voltage above 0V to see if we could increase the flipping angle. As can be seen in Figure 15, this was unsuccessful, as increasing the voltage just decreased the flip angle and moved it further from 90 degrees.

The next attempt to compensate for the incorrect angle was to increase the temperature of the liquid crystal. As shown in Figure 16, this attempt was also unsuccessful as an increased temperature moved the flipping angle further from 90 degrees once again.

Finally, we decided that the 89 degree flip would suffice and as is shown in the S3 section, the circular polarisation does not suffer greatly from the 1 degree difference.

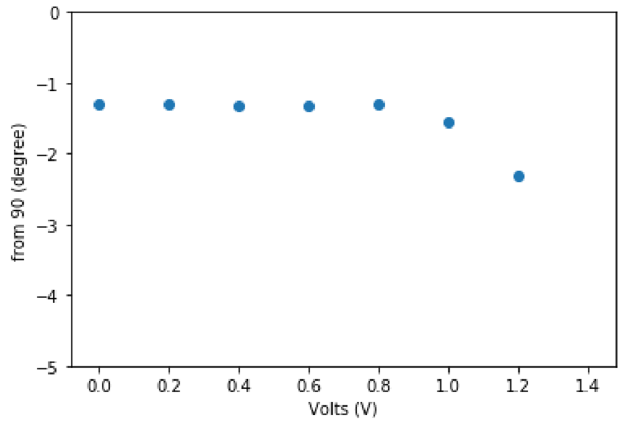

Figure 15: Voltage v. 90 degree flip to try and compensate for the 89 degree flip

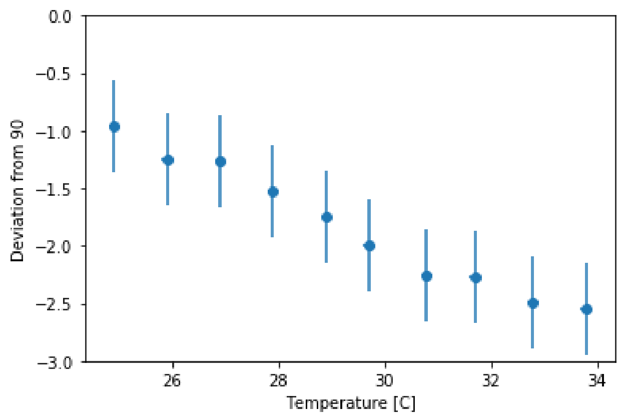

Figure 16: Temperature v. 90 degree flip to try and compensate for the 89 degree flip

5.2 Extinction time measurements

Figure 17 shows the time dependence of the extinction going from the 10V to the 0V state using the square waveform. The T.N.E. waveform cannot be used in this rotator because we are flipping from 0V to 10V and there is not possibility to overshoot past 0V. It takes about 50ms to get to the 0V state from the 10V state which is comparable to the first TNLC when it was using the T.N.E. function so we can see that we are not greatly disadvantaged by the fact that we cannot use that feature.

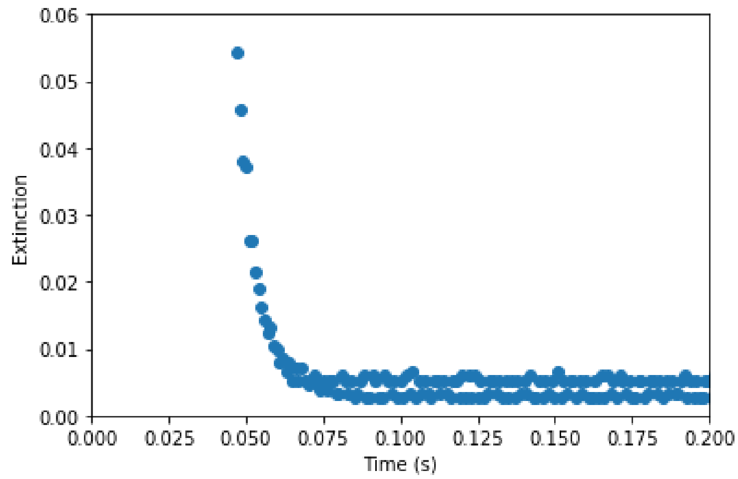

Figure 17: Extinction time going from a 10V to 0V state using a square wave function where 0s is when the voltage flipped.

5.3 Circular Polarisation v. QWP angle

5.3.1 Optimising Quarter Wave Plate

Now we need to install a Quarter Wave Plate (QWP) in order to circularly polarise the light. In order to get the best circularly polarised light, the linearly polarised light (from TNLC) into the QWP must be at 45° from the QWP fast-axis.

To optimize the QWP is rotated and the S_3 is measured for a number of angles in order to find the QWP orientation that will give the best S_3.

5.3.2 Results

Figure 18 was used to find the QWP angle that would yield the best S_3 (QWP: MDLK D2180). It is clear from the plot that the 0V and the 10V state do not have the same optimal QWP angle and this is expected since the linear polarisation flip from both states is not 90 degrees. It is also clear that the 10V state has a higher S_3 than the 0V state.

5.3.3 Handedness Bias

Since the 10V state tends to have higher extinction values and S3 values, we thought that rotating the QWP by 90 degrees would allow for a better value of S3 for the 0V state which would hopefully match up with the S3 for the 10V state. Additionally, we added a linear polarizer in between the TNLC and QWP as in Figure 19 in order to improve the quality of the linear polarisation incident on the QWP. The results showing the handedness bias are plotted in Figure 20. In both plots, the 0V state is blue and the 10V state is orange. The plots are like mirror images and show that the quarter wave plate has more retardance in one direction than the other resulting in a difference in the S_3 values in each state.

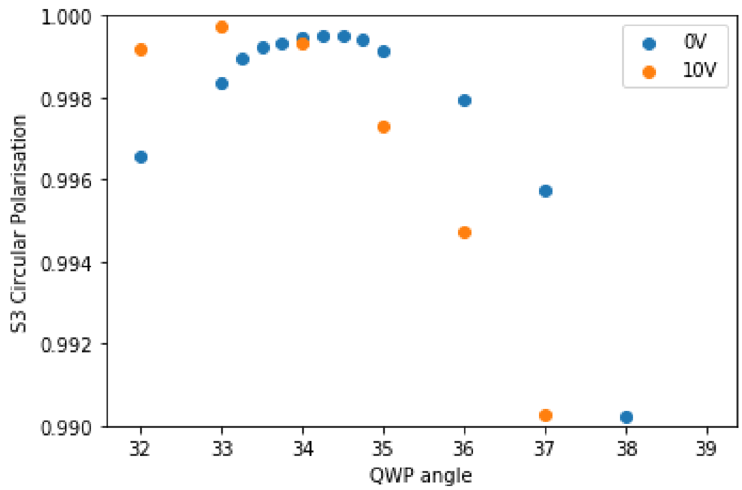

Figure 18: S_3 v. QWP angle using MDLK D2180

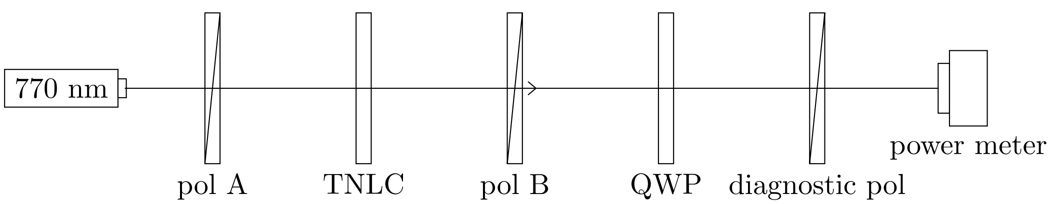

Figure 19: Setup using an additional linear polarizer B to clean up the linear polarization from TNLC

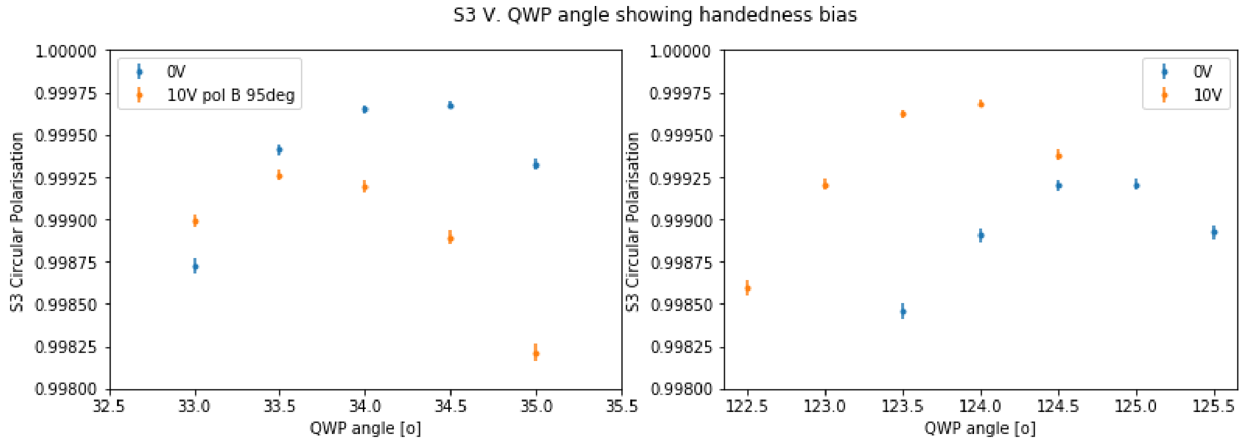

Figure 20: S_3 v. QWP angle using D2180 showing handedness bias

5.3.4 Changing the Quarter Wave plate

Having shown this handedness bias, we wanted to see if the QWPs on the trap exhibited the same effect. Figure 21 shows the results from the top trap polarizer (I12117). Once again the setup used for these measurements was the one from Figure 19. The S_3 quality in both orientations is almost equal. The right plot shows a better S_3, the best value in each case was measured to be 0.99996 in the 0V state and 0.99993 in the 10V state. It is clear however that looking at the plot that the QWP angle must be different for each state in order to achieve the best S_3, this issue is addressed in the following section with the addition of the linear polarizer.
Once again using the setup from Figure 19, the results for the bottom QWP (I12118) are shown in Figure 22. At the QWP angle of 42.5 and S_3 of 0.99996 ± 0.00003 was measured. The handedness bias is less evident here but can still be seen as the 0V state has a better S_3 than the 10V state. Note that the curves of each state over lap more that in Figure 21 because the polarizer B angle has changed. This will be further addressed in the next section.

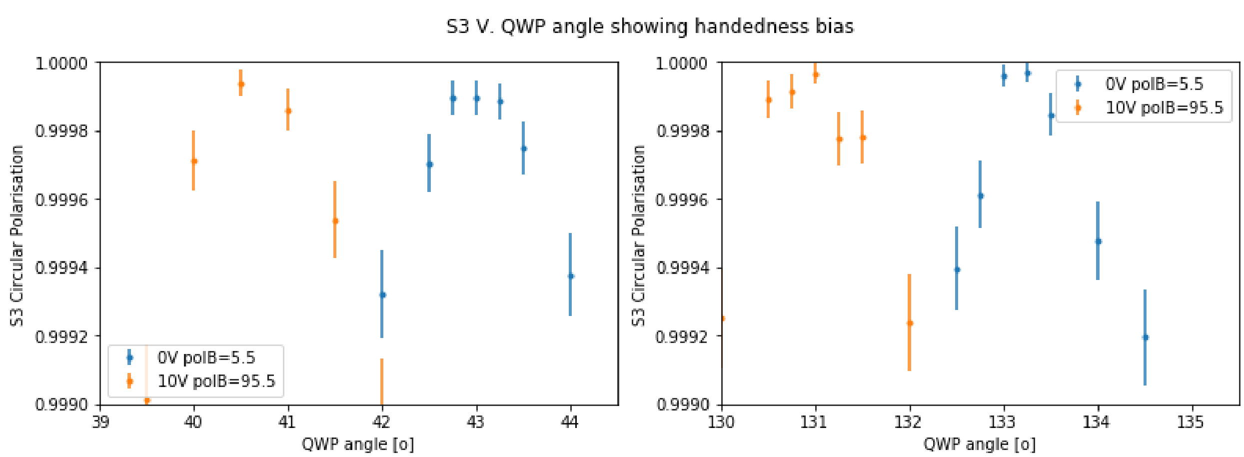

Figure 21: Top trap polarizer I12117 handedness bias test

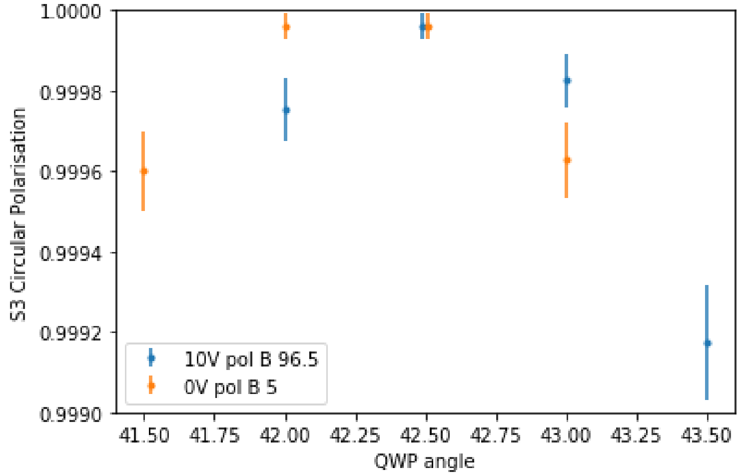

Figure 22: Bottom trap polarizer, S_3 v. QWP angle (I12118)

5.3.5 Addition of Linear Polarizer

The discussion of adding a linear polarizer in between the TNLC and the QWP as in Figure 19 began in the previous section. One of the aims of this additional polarizer was to improve the quality of the linearly polarized light. This polarizer would remove any ellipticity that might have been added to the polarisation in the TNLC and ensure only linearly polarised light went to the QWP. The second aim was to correct for the 89 degree flip that happens with this TNLC, which we saw in Figures 20 and 21 led to offsets in the best possible S_3. Finally, this additional polarizer will allow us to have confidence that the linear polarization orientation incident on the QWP is reproducible. Since we have seen that the rotation is dependent on temperature and voltage fluctuations, a linear polarizer that rotates physically between two states would ensure that even if the TNLC's rotation drifts, the linear polarisation would not be affected, only the power output would change.

We can see the benefit of having the additional linear polarizer B in the comparison of Figures 23 and 24 where the quality of S_3 was increased by an order of magnitude. The best result for the top QWP was 0.99996 ± 0.00003. The results for the bottom polarizer are shown in Figures 25 and 26, they are very similar to the top polarizer, once again with the linear polarizer the optimal S_3 was 0.99996 ± 0.00003.

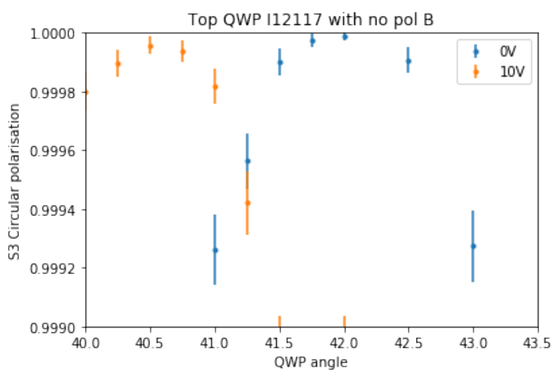

Figure 23: S3 v. QWP angle without a linear polarizer best S3 at the same QWP angle was 0.9994

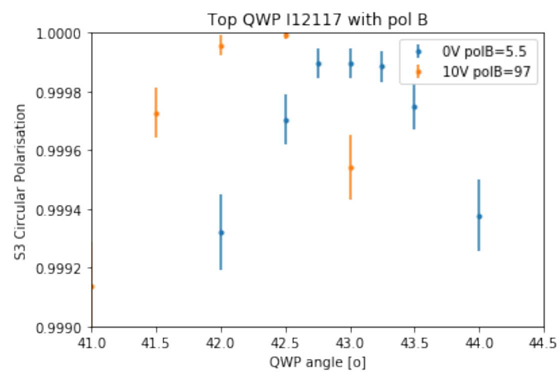

Figure 24: S3 v. QWP angle with a linear polarizer best S3 at the same QWP angle was 0.99996

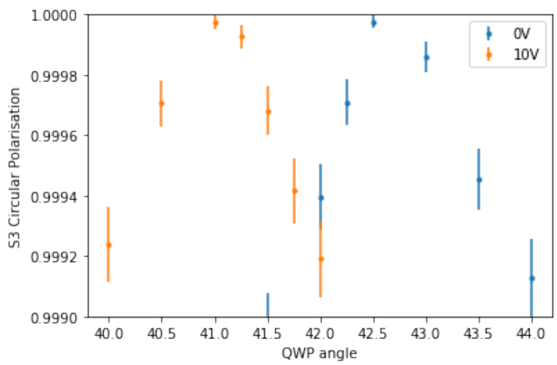

Figure 25: S3 v. QWP angle without a linear polarizer best S3 at the same QWP angle was 0.9992

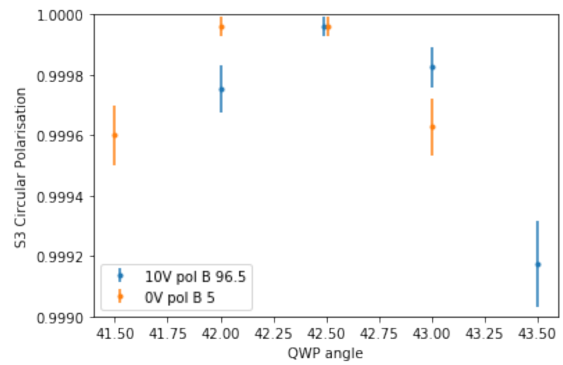

Figure 26: S3 v. QWP angle with a linear polarizer best S3 at the same QWP angle was 0.99996

5.4 Circular Polarisation as a Function of Time

The measurements for S_3 as a function of time was done with the poorer QWP the Meadowlark D2180 and are shown in Figures 27 and 28. We can see that the S_3 is not as good as was found in the previous section, this is because the poorer QWP was used, these plots therefore should be used as an indicator of the speed of the polarisation flip rather than the quality of the flip. We can see clearly from the plots that using the linear polarizer as in Figure 19 greatly reduces the time taken to flip from one polarisation state to the other. An important observation from Figure 29 is that on the seconds timescale S_3 does not drift as it did in the first TNLC. Although the linear polarizer would eliminate any effects of the drifting S_3, it is still good to note that there is no drift on the longer timescale.

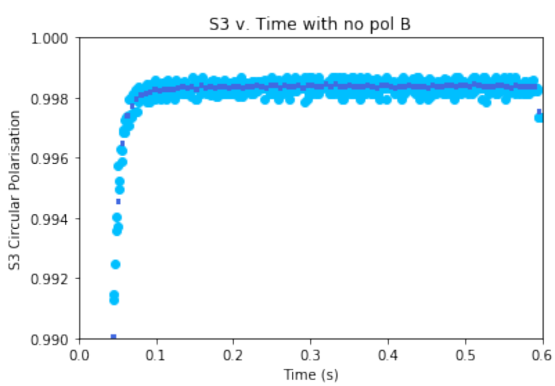

Figure 27: S3 v. time without a polarizer B using QWP: Mdlk D2180.

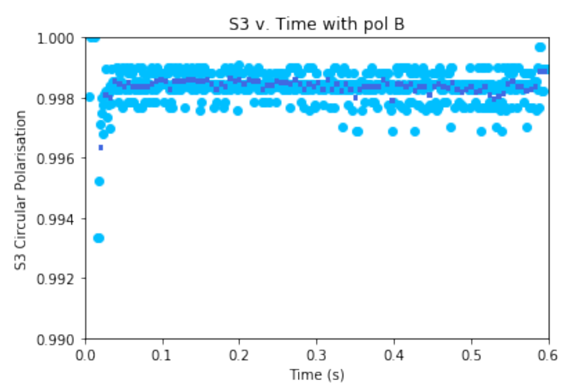

Figure 28: S3 v. time with a polarizer B using QWP: Mdlk D2180.

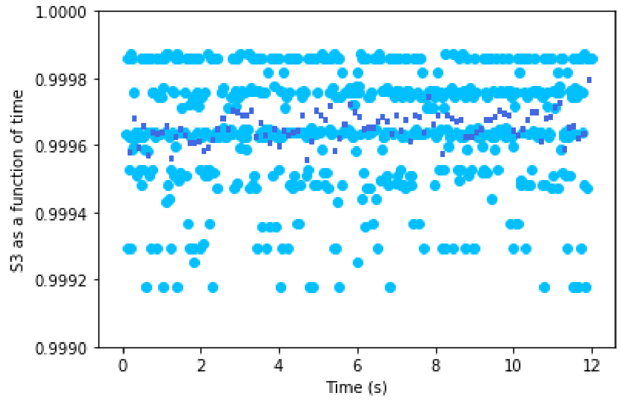

Figure 29: Longer time scale showing no drifting of S3 on a longer time scale, no polarizer B in this setup. (Using I12117)

6 Mechanics and Controls of Motorized Thorlabs Stages

6.1 ELLO Software

Controlling any of the ELL motorized devices can be done through the buttons on the circuit controller or the ELLO software provided by Thorlabs. The software can be found on the Thorlabs website (linked in References).[2] The device is connected to the computer through the USB cable provided. Once the software is opened and the device is connected through the cable, press ”Connect” in the top left corner. A controls interface will appear and is fairly intuitive. ”Jog” will move the device a set distance. ”Move Absolute” will move the device to some absolute position.

6.2 Serial Commands

Another way of controlling the device is to send serial commands. There is a communications protocol at the Thorlabs website that has a guide with commands corresponding to various controls. Before attempting to connect the device using a C++ code, I sent line commands using Moserial. To open Moserial, open up a terminal on the laptop and type “sudo moserial” which opens up an application. To find the device type “cd /dev” then “ls -lrt” in the terminal. The device should be called USB0 or USB1 or something similar. In moserial press connect in the top left corner to connect the device and input the settings given in the communication manual.[2] Once the device is connected send serial commands by simply typing into the outgoing line and pressing Send. The device will respond and the location data will be sent through the Received ASCII box in Moserial. The location data is written in hexadecimal format explained in the sections below with respect to each device.

To home the device the command is “0ho0”, the first 0 denotes the address of the device. The default address is 0. If two devices are connected, they will both have address 0. The only way I was able to change the address of one of the devices so that they could each get separate commands was to first connect one device, then change the address using the command “0ca1” which will change the address of device(s) “0” to address “1”. This way commands can be sent to individual devices.

Once the line commands were tested using Moserial I was able to send commands in a C++ code. The code I wrote can be found in the folder /aafanassieva/ellxcontrolls. The code explains the steps of connecting the devices and sending commands. There is also a link to a website that has more information on sending serial commands in C++.

One flaw of controlling two devices at the same time was that the devices can spontaneously switch addresses. On one occasion, I tried to connect two rotation stages and have them move independently of each other. One device had address “0” and the other had address “1”. I set device “0” to move between 2 positions every 10 seconds, while “1” was stationary. After a few cycles, device “1” spontaneously changed its address so that it would also begin moving between two positions as if it were device “0”. This only happened when device “1” was sent no commands while device “0” was moving. If both devices were sent different commands at the same time this problem did not occur.

6.3 ELL14 Rotation Stage

The ELL14 motorized rotation stage from Thorlabs, was initially used for diagnosis of the circular polarisation. Later, we used it for the linear polarizer in between the TNLC and the Quarter Wave Plate in Figure 19. The controls were described in the section above.

When using the rotation stage to move between two set positions it is recommended to use the "Move Absolute" function, which will rotate the stage to a set location with respect to the "home" location. The serial command to execute this command is "0ma00008C00". The first "0" should be changed to the address of the desired device. "ma" is the command for "Move Absolute". The last 8 digits give the position to which the device will be moved. In this case the device was moved to position 90°. To translate the angles to the required hexadecimal number for the command follow Equation 5. This is because there are 143 360 pulses for a 360° rotation. Then convert d to the hexadecimal number. For example

$$\theta \times \frac{143360}{360} = d \tag{5}$$

As an example, the command for a 90° position is "00008C00". The calculation is shown in (5), this is then converted to hexadecimal as 8C00.

$$(90) \times \frac{143360}{360} = 35840 \tag{6}$$

There is a code written in /aafanassieva/ellxcontrolls on the HP laptop called "twoell14.cpp" which controls two rotation stages and also reads their output positions. There is also a python code for plotting these positions which can be accessed through jupyter.triumf.ca under /trinat/aafanassieva-jupyter/Controlling and Measuring ELL devices/ ELL14 Rotation Stages.

6.4 ELL20 Linear Translation Stage

The translation stage was one of the options to be used for the linear polarizer in between the TNLC and the Quarter Wave Plate in Figure 19. The proposed design for this is shown in Figure 30. The goal was to have two linear polarizers set at two angles for the optimal circular polarisation with each Quarter Wave Plate. The device would move horizontally to allow the appropriate polarizer to enter the beam line as required.

While testing the device we found that in one direction the movement went very quickly. In the other direction the moving component was getting stuck around the middle of the track. The device overheated often and could not always move through the full range of motion. We decided that this device would not be reliable for the application required. Thorlabs cited that the device could move a maximum load of 200g, our device was 150g.

The device was controlled the same way as the rotation stage. For the hexadecimal component of the command, there are 26 010 pulses per inch. The same calculation would need to be made as in (5) but this time you would need to multiply the distance required in inches by 26 010 and then convert to hexadecimal.

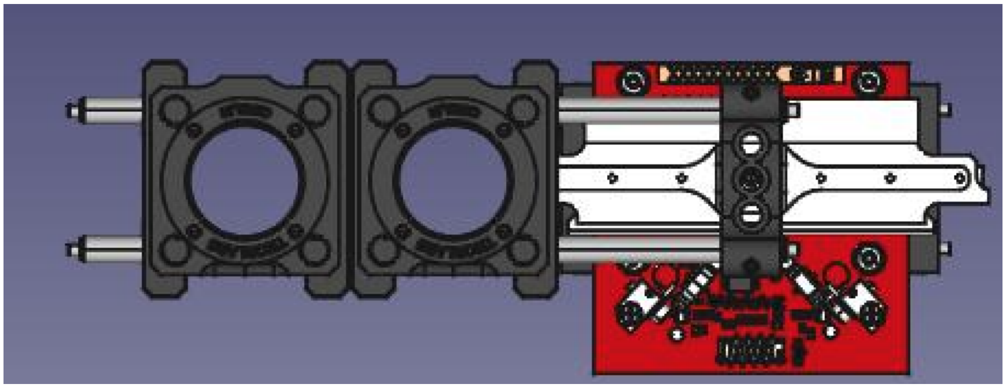

Figure 30: Set Up for Linear Translation stage

7 Optical Fiber Coupling

The optical pumping light needed to be transmitted from the initial diode laser to the atom trap using optical fibers. In order to get the light into the fiber, we use a series of two lenses with focal lengths $f_1 = 40.0$mm and $f_2 = 50.0$mm. The two lenses have two purposes: they make a telescope to optimize the diameter of the input beam, and they allow for a better focus into the fiber than can be achieved with the PAF-X-15-B fiber launcher alone. A drawing of the setup is shown in Figure 32. The third lens in the drawing is the lens in the PAF-X-15-B (new item number:PAF2A-15B) fiber input port with $f_3 = 15.4$mm. The power output was measured by using a power meter to measure the light coming out of the output port of the fiber.

In order to optimize the power transmission, we adjusted the two mirrors before the telescoping lenses. To chose the magnification and adjust the alignment, light from a fiber tester was sent the opposite way through the fiber. Using a piece of paper allowed for a comparison between the size and divergence of the incoming and outgoing beams. To further optimize the power, I turned the Z-adjust of the first lens (f_1), this changed the distance between the first two lenses (d_1). The plot shown in Figure 31 shows the power transmitted through the fiber going to the bottom arm of the trap with respect to the number of turns in the z-adjust. The 0 point on the x-axis refers to when the z-adjust was screwed in as much as possible, and one turn is equivalent to increasing the distance between the two lenses by 0.05mm. To find an equation to fit this plot, a series of lens calculations were required, and the full derivation is shown below.

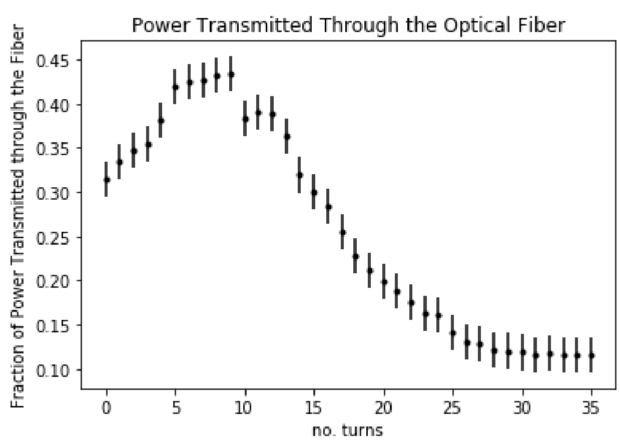

Figure 31: Ratio of the power transmitted through the fiber per no. of turns

In the process of fitting the data, there was first a simplistic fit and then one that accounted for more physics. The first fit was calculated approximating the area overlap between the fibre tip and the incoming beam waist. The second fit took into account the Gaussian intensity profile as well as the area overlap between the beam waist and the fibre tip.

The goal of the first calculation is to find the waist size of the beam at the fiber tip, which is shown in at the right of Figure 32. Once we can find the waist size at the fiber tip, we can approximate the power input as the overlap in the area of the fiber tip and the beam size. Equation

7 shows this approximation, and the maximum beam transmission would occur if the waist size of the beam is equal to the size of the fiber tip.

$$P \approx \frac{A_{fiber}}{A_{beam}} \tag{7}$$
$$P \approx \frac{\pi r_{fiber}^2}{\pi r_{beam}^2}$$
$$P \approx \frac{r_{fiber}^2}{r_{beam}^2} \tag{8}$$

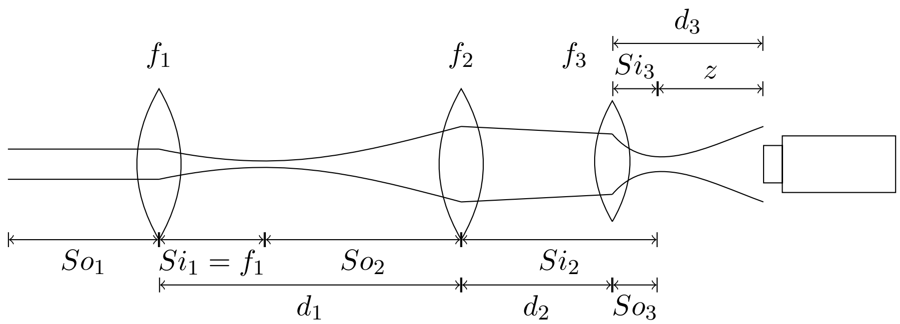

Figure 32: Figure showing all variables of the equation

To find the size of the waist at the fiber tip, we need to first solve for Si_2 as shown in Figure 33. Si_2 is the image of lens 2 and therefore the object of lens 3. Si_2 can be calculated using Equation 9. Following Figure 33, we can see that $So_2 = d_1 - Si_1$ and since the incoming beam can be approximated as parallel, $Si_1 = f_1$. Using this information we can write Equation 9 as Equation 10. Our independent variable for the fit function is d_1, since this is the variable we are changing with the z-adjust. d_1 is calculated using Equation 11 where x_0 is the initial distance in between the two lenses, n is the number of turns and $\Delta x = 0.05$mm, the distance travelled with one turn.

$$Si_2 = \frac{So_2 f_2}{So_2 - f_2} \tag{9}$$
$$Si_2 = \frac{(d_1 - f_1) f_2}{d_1 - f_1 - f_2} \tag{10}$$
$$d_1 = x_0 + n\Delta x \tag{11}$$

Once we have Si_2 calculated, the next step is to use Equation 12 to calculate Si_3. As can be seen in Figure 34, $So_3 = d_2 - Si_2$, which can be used to derive Equation 13. Note that in Equation 13, Si_2 should be the absolute value of the answer given by Equation 10 due to the sign rule. This will give an So_3 that is negative, which means that the object of lens 3 is to the right of the lens, as can be seen in Figure 34.

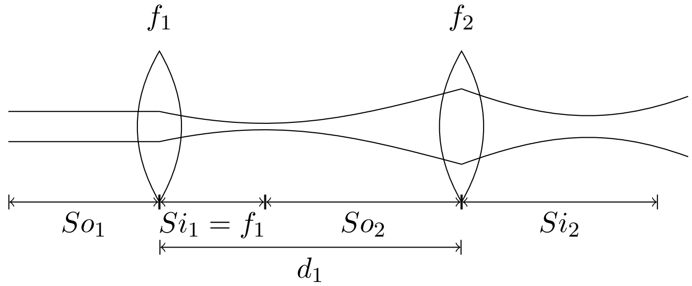

Figure 33: Figure showing the first step's variables

$$Si_3 = \frac{So_3 f_3}{So_3 f_3} \tag{12}$$

$$Si_3 = \frac{(d_2 - Si_2) f_3}{d_2 - Si_2 - f_3} \tag{13}$$

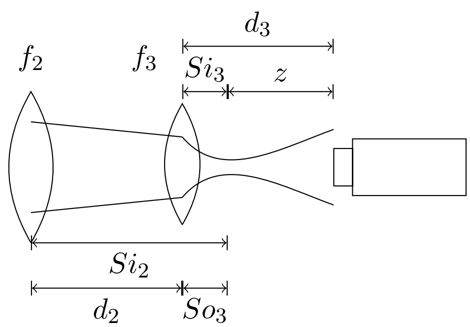

Figure 34: Figure showing the final step's variables

To calculate the waist size at the fiber tip, we need to know the value of z. As shown in Figure 34, z can be calculated with Equation 14 using the value of Si_3 from Equation 13 and $d_3 = 15.4$mm from the Thorlabs manual.
We can then use z to solve for the waist size w using Equation 15. λ is the wavelength of the light (770nm or 0.00077mm), w_0 is the minimum waist size of the beam.

$$z = d_3 - Si_3 \tag{14}$$

$$w(z) = w_0 \sqrt{1 + \left(\frac{\lambda z}{\pi w_0^2}\right)^2} \tag{15}$$

I fit the data set using the lens equations shown above, using the optimize function from python's scipy library, and set w_0 as the unknown variable. The resulting plot is shown in Figure 35, where w_0 was found to be 0.004mm. The fit is clearly not perfect because the data flattens out around

0.10. The fit does not account for this, but it still gives an idea of how the power should behave as the distance between the two lenses changes. Using the result from the fit, we can also solve for the Rayleigh range given Equation 16. The Rayleigh range is defined as the the distance along the direction of propagation where the area of the beam doubles. In other words, where the waist size is equal to $\sqrt{w_0}$. The Rayleigh range was found to be $z_R = 0.07$mm.

$$z_R = \frac{\pi w_0^2}{\lambda} \tag{16}$$

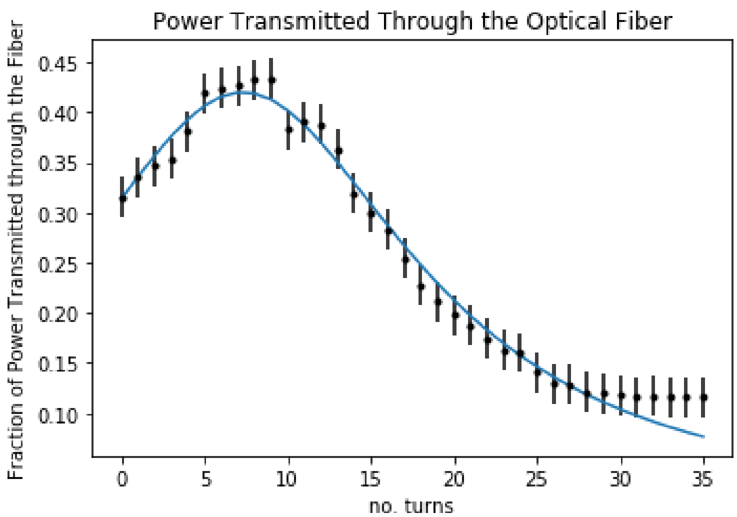

Figure 35: The percentage of the power transmitted fitted using the lens calculations and floating w_0

The fit in Figure 35, only took into account the area over lap of the incoming beam and the fibre tip. To try to get a better fit, I had to try to account for the Gaussian intensity profile along the radial direction of the beam. Meaning, taking into account the fact that the center of the beam is the brightest spot and the light diffuses from there. The equation for the light intensity with respect to the radius from the center is shown in Equation 17.

$$I(r, z) = I_0 \left(\frac{w_0}{w(z)}\right)^2 \exp\left(\frac{-2r^2}{w(z)^2}\right) \tag{17}$$

The python code I used to fit this function can be found in trinat's trcomp account in the folder /aafanassieva-jupyter/optical fibre/Fibre Launching Fit and can be accessed by going to jupyter.triumf.ca and signing in using the username trinat and the trinat password. The function that was used to fit the data is shown in Figure 36. It takes as input z which is calculated for each value of the "no. turns" using Equations 9 - 14. The parameters w_0 and a were optimized using the scipy.optimize library, and w_0 corresponds to the waist size of the beam as discussed previously, while a is the scaling factor for the function.

The first line in this function definition simply expresses Equation 17, where r is the distance radially outward from the center of the beam and $\_z$ is the distance away from the minimum beam waist. The reason I use $\_z$ when writing out this function is so that the code can differentiate between the data points stored as z and the variable in the equation z. The code gets confused when trying to integrate the equation if done differently. The second line of code integrates $I(r, z)$ from 0 to $w(z)$. This is done to normalise the function, since the waist is defined to be the area where the 2σ point is on a Gaussian distribution, roughly 95% of the intensity is contained within the waist. The argument "for $\_z$ in z" allows the function to be integrated for every data point z and "norm" is now an array of values. The third line divides 0.95 by "norm" to create an array "factor" of constants that will be used to scale the second integral appropriately.

The second integral in this calculation called "integral", now integrates the same function but this time from 0 to the radius of the fibre tip. Finally the normalising factor is multiplied by the second integral and this gives of a measure of the ratio of the power transmitted through the fibre.

```
def func(z,w0,a):
    fn = lambda r,_z :  ((w0/waist(_z,w0))**2)*exp((-2*r**2) / (waist(_z,w0))**2)
    norm = np.asarray([integrate.quad(fn, -waist(_z,w0), waist(_z,w0),args=_z)[0] for _z in z])
    factor=0.95/norm
    integral=np.asarray([integrate.quad(fn,-tipsize,tipsize,args=_z)[0] for _z in z ])
    powergauss=factor*integral
    return powergauss*a
```

Figure 36: Function used to fit the data incorporating the Gaussian intensity distribution from Equation 17

The result is shown in Figure 37. The orange line represents the fit found using this second method where the Gaussian intensity profile was taken into account. The blue line shows the same calculation as in Figure 35 where we only took into account the Gaussian waist shape of the beam and the area overlap between the beam and the fibre tip. The orange fit looks better than the blue one, although it still does not completely account for the flattening out at the right side of the plot above 28 turns. When I tried to add an offset to the fits, the blue fit gave me an offset of zero while the orange fit tried to give a negative offset and didn't fit the function much better so I removed the offset feature. With or without the offset the values for the w_0 and a where very similar.

For the orange fit, $w_0 = 0.0019 \pm .0001$mm and $a = 0.459 \pm 0.002$. The w_0 is about half of the value given by the blue fit and a is also half of that of the blue fit where the scaling factor a was 1. The w_0 given by the second fit makes more sense than that of the first fit because if we take $w_0 = 0.002$mm and do a waist calculation for $w(z)$ at $z = 15.4$mm, we find that the waist size at f_3 is 1.89mm and the diameter of the beam is 3.77mm. If we take this to be approximately the size of the beam at f_2 which is reasonable due to the parameters shown in Figure 34, and do a magnification calculation given the focal lengths of f_1 and f_2 we find that the beam incoming into f_1 should be approximately 3.02mm. When I measured the beam diameter by eye it was about 2.8mm. If we do the same calculation for $w_0 = 0.004$mm we find that the incoming beam diameter is 1.5mm which is not a realistic beam size.

The fact that the fit does not allow for the flat tail at the right hand end of the plot could perhaps be an indication that our laser is not a perfect TEM00 laser. The laser going into the first lens was also quite elliptical in shape rather than a circle, which could be another reason this fit does not work perfectly. We found that when we used an anamorphic prism to try and round the elliptical shape by expanding the shorter axis, we lost a lot of power and were not able to get as much transmission through the fibre. We are not sure why this did not help, since we tried two telescope version to optimize the resulting beam size. We believe the ingoing beam is not astigmatic, so this will not change the functional form in Fig. 5, but will change the normalizations. I tried to find a way to account for the divergence angle going into the fiber as well to see if that would help the fit. The Thorlabs manual for the fibre launcher cites the values for the divergence angle and the numerical aperture of the launcher. I was, however, unable to find a way

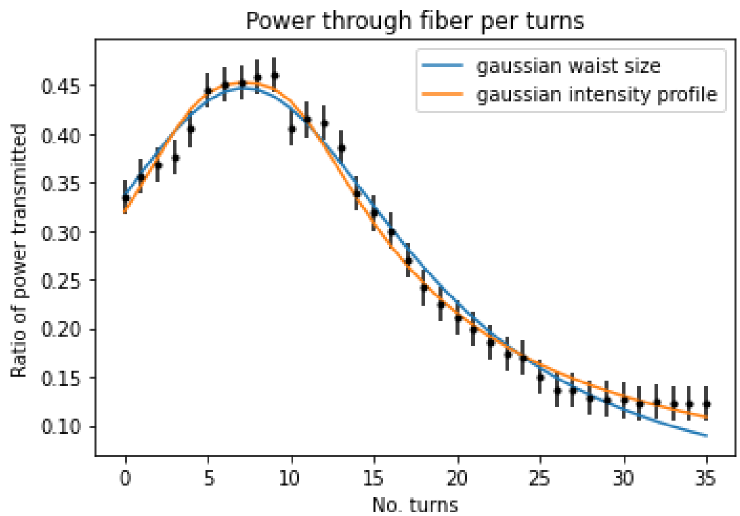

Figure 37: Fitting the optical fibre transmission plot with the Gaussian intensity profile incorporated into the equation shown by the orange fit.

The best power through the optical fibers are shown in the table below. The input power was measured before the telescoping lenses and the output power was measured at the output end of the fiber. The measurements were made using a handheld power meter. The laser diode had been changed before making these measurements. The total power available into these two fibers is about 8mW. (The ingoing beam was optimized in each of the measurements for convenience and accuracy of the power reading scale.) The previous power transmission was closer to 1/3 (see Scott Smale's co-op report for details), so the new diode has improved both the fiber transmission and the total power available by nearly a factor of 10.

Beam	Input Power (mW)	Output Power (mW)	Fraction
top	1.86	1.04	56%
bottom	2.40	1.01	42%

8 Simulating Nuclear Spin

Now that the power and the circular polarisation of the optical pumping beam have improved, it is important to see the resulting improvement of the nuclear spin polarisation. To find a theoretical result for the nuclear spin polarisation improvement, I used Ben Fenker's Optical Bloch Equations code. [1] I compared the previous setup using an S_3 of 0.995 to the new S_3: 0.9995. Note that this 0.9995 is taken from Figure 4 in Claire Warner's Co-op Report and the known birefringence of the viewports. [4] The figure was used to approximate the value of S_3 inside the atom trap given an input S_3 of 0.99996.

Figure 38 shows Nuclear Spin Polarisation calculated by the Optical Pumping simulation with respect to time. The red and green curves show the nuclear spin polarisation with an $S_3 = 0.995$ while the blue and orange curves show the same for an $S_3 = 0.9995$. The blue and green curves show the values for nuclear spin polarisation with 3x power while the orange and red curves show those with 1x power.

The improvement in power transmitted to the optical pumping light shows a significant decrease in the time it takes to achieve a stable nuclear spin polarisation. This means that there is more time to take good data in the beta asymmetry measurement. The nuclear spin polarisation improved from a final state of 0.9958 to a state of 0.9970. As a check to see the best possible polarisation given the parameters of the trap (magnetic field laser power), I ran a test setting S_3 to 1. This gave a nuclear spin polarisation of 0.9970. This tells us that the limiting factor for the nuclear spin polarisation is not the circular polarisation of the light. The limiting factor of the nuclear spin polarisation is now the Larmor Precession fighting the optical pumping.

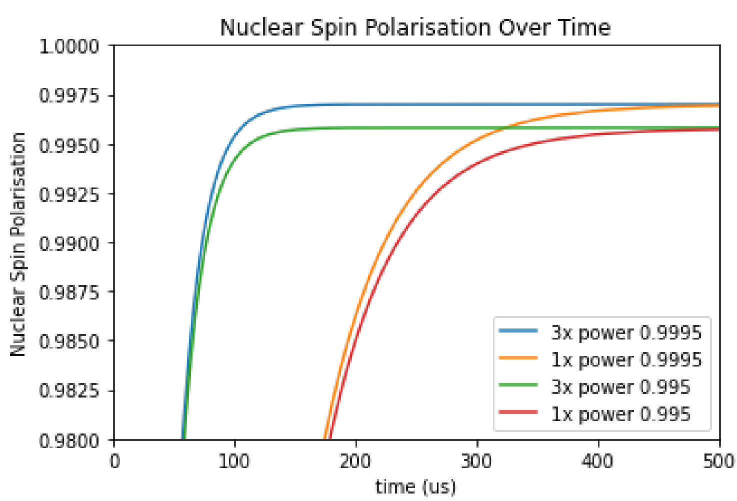

Figure 38: Optical Bloch Equation Simulations of Nuclear Spin Polarisation

9 Conclusion and Next Steps

Over the course of the term I was able to characterize the TNLCs and improve the circular polarisation of the optical pumping light. I was able to design and test a new setup with an additional linear polarizer in between the TNLC and the quarter wave plate which greatly improved the quality and reliability of the circularly polarised light.

What needs to be done next is to implement the design onto TRINAT. The two TNLCs need to be placed on the trap arms. The quarter wave plates need to be reinstalled and optimized given the new TNLCs which almost surely will not have the same optimal angles as did the LCVRs which are presently mounted on the trap. One would also need to work out the best way to test the circular polarisation of the light on the trap itself once all the components are in place, most likely using a motorized rotation stage.

References

[1] Ben Fenker. Optical bloch equations. Apr 2015.

[2] Thorlabs Inc. Ello software. https://www.thorlabs.com/software_pages/viewsoftwarepage.cfm?code=ELL.

[3] Meadowlark Optics. Twisted nematic liquid crystal binary rotator.

[4] Claire Warner. Pctfe as a solution to stress-induced birefringence in atom trap viewports. *TRINAT Co-op Report*, Apr 2014.